Scientific Research Publishing

Advances in Materials Physics and Chemistry, 2022, 12, 19-32
https://www.scirp.org/journal/ampc
ISSN Online: 2162-5328
ISSN Print: 2162-531X

Study on the Physical and Mechanical Properties of Al-Powder Reinforced Bioactive Glass: Ceramic Composite Material

Muhammad Hafizur Rahman Khan[1*], Sazzad Hossain[2*], Mohammad Maksudur Rahman[2*]

[1]Department of Physics, International University of Business Agriculture and Technology, Dhaka, Bangladesh
[2]Department of Physics, Jahangirnagar University, Savar, Dhaka, Bangladesh
Email: sazzadju41@gmail.com, likhon_phy@yahoo.com

How to cite this paper: Khan, M.H.R., Hossain, S. and Rahman, M.M. (2022) Study on the Physical and Mechanical Properties of Al-Powder Reinforced Bioactive Glass: Ceramic Composite Material. *Advances in Materials Physics and Chemistry*, **12**, 19-32.
https://doi.org/10.4236/ampc.2022.122002

Received: January 17, 2022
Accepted: February 25, 2022
Published: February 28, 2022

Abstract

Glass-ceramic samples, having composition of SiO_2-35, CaO-45, Na_2O-10 and P_2O_5-10 in weight ratio were prepared through sintering route. Glass powder was reinforced by Al powder. The strength of glass-ceramic composite was found to be temperature dependent, and it varies with the addition of Al powder. Flexural strength increases with the increase of powder addition and sintering temperature, however, decreases with the increase of sintering time. There is an optimum temperature (>1100˚C) above which flexural strength of all samples decreases. Bulk density changes to a higher value as the addition of Al-powder increases up to 3% by weight above which density decreases slowly. On the other hand, apparent porosity and water absorption decrease with the increase of percentage of Al powder added. Porosity and water absorption also showed a dependent characteristic on sintering time and sintering temperature.

Keywords

Biomaterials, Glass Ceramics, Aluminum Powder, Composite Material

1. Introduction

Biomaterials have been drawn much attention in the recent time due to their extensive medical and non-medical uses [1] [2]. Bioactive materials, when used in a medical device, may interact with the biological systems. They can react in a positive manner with the local cells to form bonds and can transfer loads to and from living cells [1] [3]. Bioactive ceramic is an important biomaterial which is

*Contributed equally.

mainly used for the replacement of damaged or diseased body parts [4]. The bioactive ceramics can perform their function within the human body without toxicity and can generate a positive reaction in the biological environment of the implants [4] [5]. Bioactive ceramics have two main classes—Bioactive glass (e.g., Bioglass) and Bioactive glass-ceramics (e.g., A/W glass-ceramic). The bioactive glasses are the third-generation biomaterials which can be employed to repair and rebuild damaged tissues, particularly hard tissues [6] [7]. Usually, SiO_2, Na_2O, CaO, and P_2O_5 are the base components of the most common type of bioactive glasses. The bioactive glasses are soft in nature and hence their final shape can be easily given [7]. The main advantage of bioactive glass is the high superficial speed reaction that brings rapid connections to the tissues. But the greater disadvantages are the not optimal mechanical properties and the meager breaking resistance. However, these disadvantages can be overcome by forming bioactive glass-ceramic from the parent bioactive glass through the process of controlled heat treatment above its crystallization temperature [8] [9] [10] [11]. The newly formed bioactive glass-ceramic possesses superior mechanical properties, including greater elastic modulus, failure strength, and hardness, than the parent bioactive glass [8] [12] [13]. However, the brittleness and low fracture toughness of bioactive glass-ceramics sometimes appear as a limitation of their common clinical uses [12]. This discrepancy again can be solved by the addition of a ductile, metallic, secondary phase to the pure glass-ceramic composite structure. Several researchers have already worked with the development of glass-ceramic matrix composites reinforced with graphite [14] [15], alumina fibers [16], SiC [17], carbon nanotubes [18], etc. In the present research work, pure aluminum (Al) has been selected as the reinforcement material due to its non-toxicity, lower density, and better ductility [19]. The resultant change on the physical and mechanical properties of the prepared glass-ceramic composite samples due to the addition of pure aluminum (Al), and the effect of sintering time and sintering temperature on the samples have been studied through this research work as well.

2. Experimental Details

The formation and evaluation of Al-powder reinforced bioactive glass-ceramic composite material was performed with six process steps as shown in **Figure 1**,

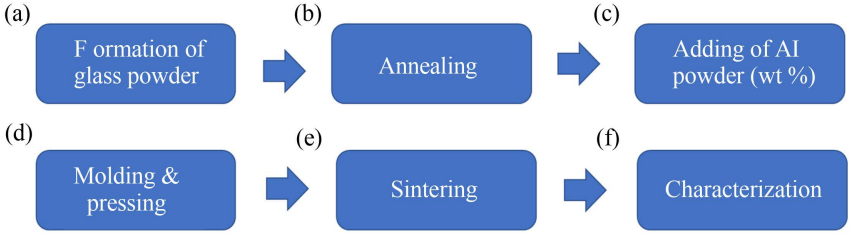

Figure 1. Process flow of formation and evaluation of Al-powder reinforced bioactive glass-ceramic composite material.

which starts from: 1) formation of glass powder; 2) annealing; 3) mixing the Al powder; 4) molding and pressing; 5) sintering, and finally; 6) checking the mechanical properties. The whole process is explained as below.

2.1. Formation of Glass Powder

In order to form glass powder, we took 500 gm glass, 175 gm of SiO_2, 50 gm of P_2O_5, 85.484 gm of Na_2CO_3 (source of Na_2O), and 401.786 gm of $CaCO_3$ (source of CaO) and mixed them properly. After mixing the compounds the mixed batch was annealed at 1135˚C in a globular furnace (heat rate several hundred ˚C per hour) for three hours to form the desired glass-ceramic matrix structure. The glass was then crushed, and the glassy powder was prepared.

2.2. Mixing of Aluminum (Al) Powder

Mixing was a vital part of this experiment. Pure Al powder was mixed homogeneously with the prepared glass powder by varying its weight (wt) percentage (%) of 0%, 3%, and 6%, respectively.

2.3. Molding and Pressing

A molding device was used to mold the mixture of Al powder and glass-ceramic powder. In this molding process, polyvinyl alcohol was used as the binder such that five drops of the binder were poured in three grams of the mixture. After then the mixture was pressed with sufficient load of 50 KN, applied by a Weber Pressen Hydraulic Press, to get the desired shape (60.5 mm × 5.5 mm × 4.4 - 4.6 mm) of the sample.

2.4. Sintering of the Samples

The samples prepared by the Weber Pressen Hydraulic Press were removed and dried properly. Finally, the dried samples were sintered at various temperatures (1050˚C, 1075˚C, 1100˚C) using high temperature furnace.

2.5. Characterization of the Samples

In the present work ASTM D790M, 3 points loading technique has been used to estimate the values of flexural strength or flexural stress (σ_f), flexural strain (ε_f), and flexural or bending modulus (E_f). In this arrangement, the flexural strength of the prepared glass-ceramic samples was determined by using the following formula [20] [21],

$$\sigma_f = \frac{3PL}{2bd^2}\left(\text{MPa}\right) \tag{1}$$

where P denotes the load at a given point on the load-deflection curve (expressed in N), L is the distance between the centers of the support span (expressed in mm), b is the width, and d is the depth (both measured in mm) of the specimen. The flexural strain was measured by the following expression [21],

$$\varepsilon_f = \frac{6Dd}{L^2}(\text{mm/mm}) \tag{2}$$

where D denotes the maximum deflection of the center of the beam (measured in mm). Also, the flexural modulus of the samples was determined by using the following equation [21],

$$E_f = \frac{L^3 m}{4b^3 d^3}(\text{MPa}) \tag{3}$$

where m is the gradient (*i.e.*, slope) of the initial straight-line portion of the load deflection curve (expressed in N/mm).

ASTM C135-762 technique has been used to determine the bulk density (BD) of the samples. The bulk density is given by the following equation [20],

$$BD = \frac{W_d}{V}\left(\text{gm/mm}^3\right) \tag{4}$$

where W_d determines the weight of the specimen (expressed in gm), and V represents the volume of the specimen under test (measured in mm^3).

The apparent porosity (P) of the samples has been determined by employing the evacuation method. The following equation [20] was used to calculate the apparent porosity,

$$P = \frac{100\left(W_s - W_d\right)}{V} \tag{5}$$

where W_s denotes the saturated weight, and W_d denotes the dry weight of the sample (both measured in mg), V is the volume of the sample (expressed in mm^3).

The water absorption is another important parameter which has been estimated by using ASTM C 67 - 91 technique. The following formula [20] provides the water absorption of the samples,

$$\text{Absorption}\% = \frac{100\left(W_s - W_d\right)}{W_d} \tag{6}$$

3. Results and Discussion

3.1. Flexural Strength

Figure 2 shows the flexural strength (σ_f) characteristic by changing sintering temperature for the glass-ceramic samples prepared with the addition of different Al powder contents: 0 wt%, 3 wt% and 6 wt%, respectively. The corresponding values of σ_f are shown in Table 1.

It is seen that the σ_f increases (5 to 9 MPa for 0 wt%, 10 to 11 MPa for 3 wt% by increasing the sintering temperature 1050˚C to 1100˚C. This cause of increasing σ_f with increasing temperature is that the strain capacity of the samples increases with the rise of temperature, and vice versa. However, σ_f decreased from 15 to 11 MPa for of Al content of 6 wt% with increasing temperature 1050˚C to 1075˚C and then little increased (14 MPa, even it is lower the value of

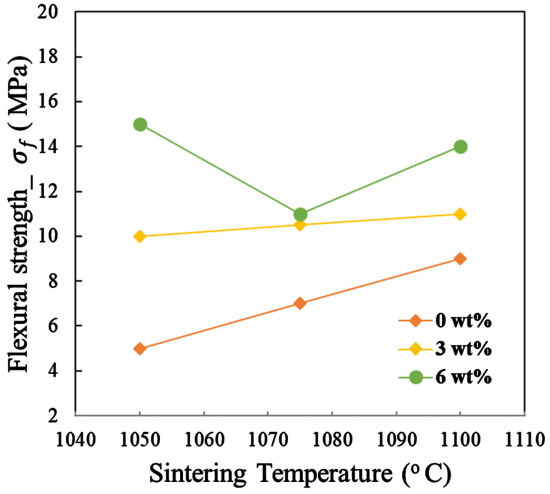

Figure 2. The flexural strength (σ_f) property of the glass-ceramics at different sintering temperature for different Al wt%.

Table 1. Flexural strength (σ_f) data of the glass-ceramics at different sintering temperature for different Al wt%.

Temperature (˚C)	Flexural strength (σ_f) (MPa)		
	Al (wt 0%)	Al (wt 3%)	Al (wt 6%)
1050	5	10	15
1075	7	10.5	11
1100	9	11	14

σ_f at 1050˚C) at high temperature of 1100˚C. It clarifies that for each temperature/percentage of oxide there is an optimum temperature/percentage of oxide amount above which the strength will be decreased. The cause of this decreasing fusion. The higher amount of Al powder lower is the fusion temperature [22].

The effect of sintering time (1.5 h and 3 h) on the σ_f for these glass-ceramic samples for different Al powder contents, 0 wt%, 3 wt% and 6 wt% as shown in Figure 3. The values of σ_f are shown in Table 2. From Figure 3, and Table 2, it could be revealed that the σ_f of the samples increases with increasing the sintering time.

3.2. Flexural Strain

The resultant change in the flexural strain (ε_f) of the composite glass-ceramic samples with different sintering temperatures has been shown in Figure 4 and the corresponding data are shown in Table 3. We observed that by increasing the sintering temperature from 1050˚C to 1070˚C, ε_f increased from 0.0028 to 0.0036 for Al wt 0%, and 0.0031 to 0.0033 for Al wt 3%, respectively. However, both ε_f for 0 wt% and 3 wt% started to be decreased by increasing the sintering temperature to 1100˚C. For Al 6 wt%, ε_f (0.029 - 0.031) was found to be almost constant at low to high sintering temperature of 1050˚C - 1100˚C. Since stress

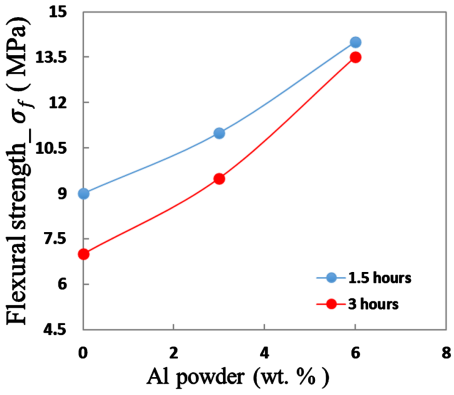

Figure 3. The flexural strength (σ_f) property of glass-ceramics at Al wt% for different sintering time.

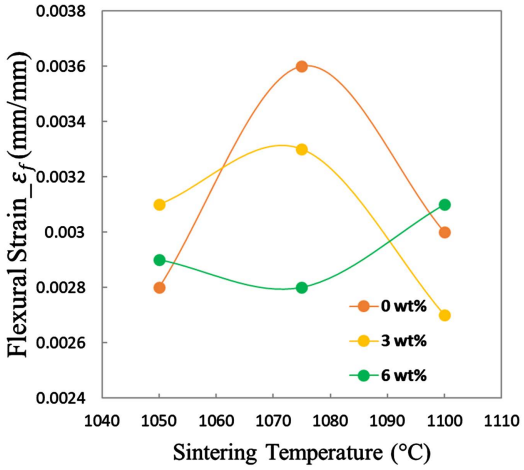

Figure 4. Flexural strain (ε_f) character of the glass-ceramics at different sintering temperature for different Al wt%.

Table 2. Flexural strength (σ_f) data of glass-ceramics at Al wt% for different sintering time.

Al (wt%)	Flexural strength (σ_f) (MPa)	
	Sintered 1.5 h	Sintered 3 h
0	9	7
3	11	9.5
6	14	13.5

Table 3. The value of flexural strain (ε_f) of the glass-ceramics at different sintering temperature for different Al wt%.

Temperature (˚C)	Flexuring strain ε_f (mm/mm)		
	Al (wt 0%)	Al (wt 3%)	Al (wt 6%)
1050	0.0028	0.0031	0.0029
1075	0.0036	0.0033	0.0028
1100	0.003	0.0027	0.0031

and strain needs to follow a proportional relationship, it is revealed that sintering temperature should be kept below 1080˚C.

3.3. Flexural Modulus

Figure 5 shows the variation of flexural modulus (E_f) with sintering temperature for the glass-ceramic composite samples prepared by adding different Al contents. The values of E_f are summarized in Table 4. It is seen that E_f for the glass-ceramics with Al wt. 6% decreased, 2700 MPa to 2200 MPa and for wt 3% decreased 2200 MPa to 1800 MPa by increasing sintering temperatures 1050˚C - 1100˚C. However, an opposite characteristic of E_f which started to be increased (1180 MPa - 1850 MPa) with increasing the sintering temperature (1080˚C - 1100˚C) was observed for the sample where no Al content was added (0 wt%). The flexural modulus of this sample with Al wt. 0% starts to increase little after a certain sintering temperature (1050˚C - 1080˚C). This discrepancy may be resolved by keeping the sintering temperature within 1080˚C which showed similar characteristics (E_f decreased by increasing temperature 1050˚C to 1080˚C) for 3 samples.

Influence of changing sintering time on E_f after adding different Al powder (wt%) is exhibited in Figure 6 and the values of E_f are shown in Table 5. The E_f

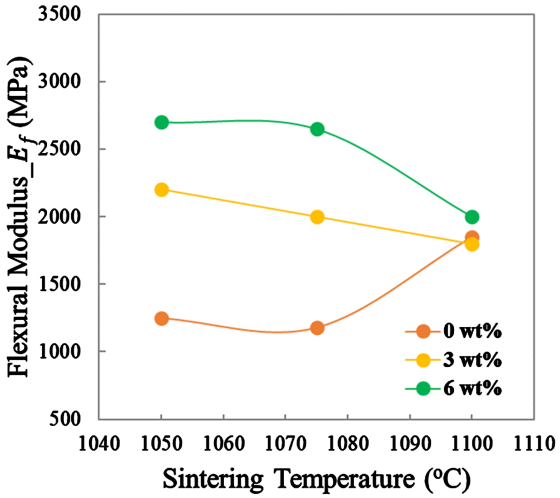

Figure 5. Flexural modulus (E_f) of the glass-ceramics at different sintering temperature for different Al wt%.

Table 4. Flexural modulus (E_f) data of the glass-ceramics at different sintering temperature for different Al wt%.

Temperature (˚C)	Flexuring modulus E_f (MPa)		
	Al (wt 0%)	Al (wt 3%)	Al (wt 6%)
1050	1250	2000	2700
1075	1180	2000	2650
1100	1850	1800	2000

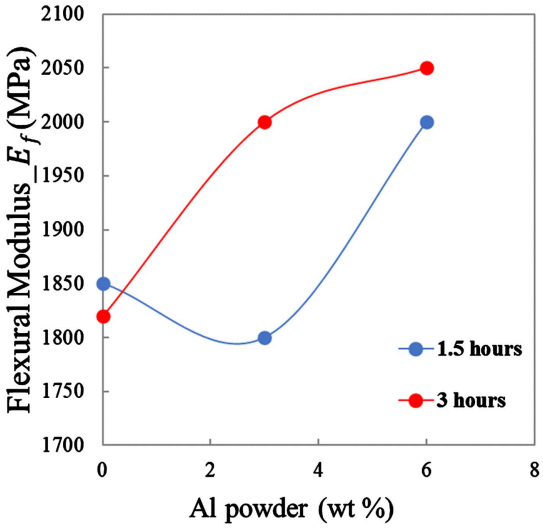

Figure 6. Flexural modulus (E_f) curves of the glass-ceramics at Al wt% for different sintering time.

Table 5. The values of E_f of the glass-ceramics at Al wt% for different sintering time.

Al (wt%)	Flexuring modulus E_f (MPa)	
	Sintered 1.5 h	Sintered 3 h
0	1850	1820
3	1800	2000
6	2000	2050

was found to be increased, *i.e.*, for Al 3 wt% 1800 to 2000 and for Al 6 wt% 2000 to 2050 MPa at sintering time of 1.5 h and 3 h, respectively. However, for Al wt 0% it is almost constant (~1800 MPa).

3.4. Bulk Density

Impact of sintering temperature on the bulk density of the glass-ceramic samples after the addition of different Al wt% is represented in **Figure 7** and their corresponding values of bulk density (BD) are summarized in **Table 6**. It is observed that the bulk density increased with increasing sintering temperature for the samples prepared with the addition of 0 wt% (2.1 to 2.25 gm/mm^3) and 3 wt% (2.15 to 2.5 gm/mm^3) of Al powders, however for the samples with Al 6 wt% decreased at a certain minimum value (2.25 to 2.18 gm/mm^3) and again increased (2.18 to 2.4 gm/mm^3) by changing the sintering temperature 1050˚C to 1100˚C. The similar result was observed in the flexural strength vs sintering temperature diagram (**Figure 2**). The relationship between flexural strength and bulk density is shown in **Figure 8**. This figure specifies that the flexural strength of the sintered glass-ceramic composite samples maintains a proportional relationship (in most cases the flexural strength becomes higher by increasing the bulk density) with their bulk density [23].

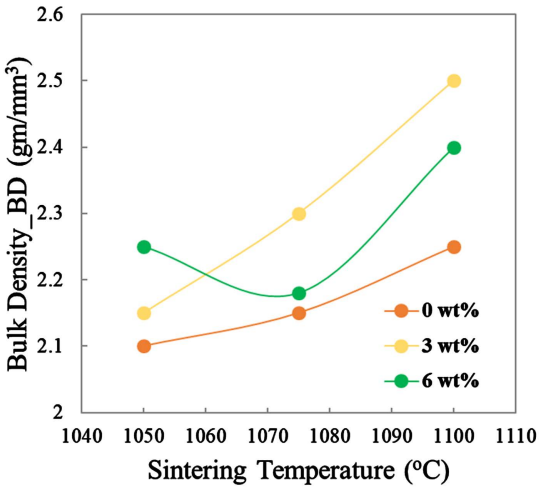

Figure 7. Bulk density (BD) characteristics of the glass-ceramics at different sintering temperature for different Al wt%.

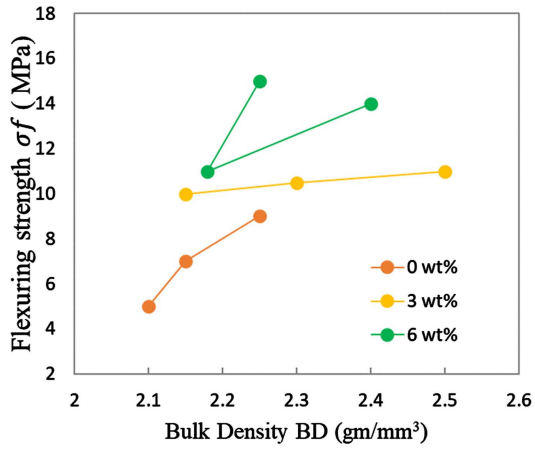

Figure 8. Flexural strength vs Bulk density graph of the glass-ceramics at different Al wt%.

Table 6. The value of bulk density (BD) of the glass-ceramics at different sintering temperature for different Al wt%.

Temperature (˚C)	Bulk Density BD (gm/mm³)		
	Al (wt 0%)	Al (wt 3%)	Al (wt 6%)
1050	2.1	2.15	2.25
1075	2.15	2.3	2.18
1100	2.25	2.5	2.4

3.5. Apparent Porosity

Figure 9 shows how the apparent porosity of the glass-ceramic composites varies with the sintering temperature. The summarized apparent porosity values are shown in Table 7. It is seen that the apparent porosity of glass-ceramics decreased (25.5 to 16 for 0 wt%, 30 to 16.5 for 3 wt%, and 27.5 to 26 for 6 wt% with

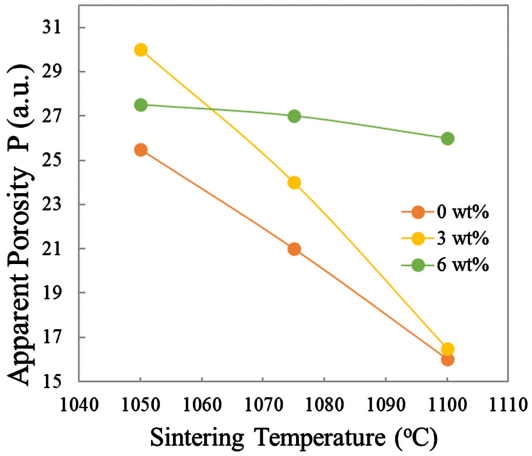

Figure 9. Apparent porosity of the glass-ceramics at different sintering temperature for different Al wt%.

Table 7. The values of apparent porosity of the glass-ceramics at sintering temperature for different Al wt%.

Temperature (˚C)	Apparent Porosity *P* (a.u.)		
	Al (wt 0%)	Al (wt 3%)	Al (wt 6%)
1050	25.5	30	27.5
1075	21	24	27
1100	16	16.5	26

increasing temperature (1050˚C to 1100˚C). However, the apparent porosity is found to be decreased less slowly for the sample with 6 wt% of Al powder. The reason behind the decrease of apparent porosity with sintering temperature is that the surface viscosity of particles of the samples decreases at high temperature and therefore the particles within the ceramic body bond more strongly and the space between the particles gets narrowed [24] [25].

The variation of apparent porosity with the percentage of Al powder at two different sintering times (1.5 h and 3 h) are shown in **Figure 10** and **Table 8**. It elucidates that both higher percentage of Al powder and long sintering time influences to increase the apparent porosity of the samples.

3.6. Water Absorptions

Continuous change of water absorption with sintering temperature is represented in **Figure 11** and **Table 9**. The water absorption curves of the composites are found to be decreased (14% to 11% for 0 wt%, 12% to 7% for 3 wt%, and 13.5% to 9% for 6 wt%) gradually with increasing sintering temperature (1050˚C to 1100˚C). This indicates that the increase of sintering temperature decreases the amount of water absorbed by the specimen, keeping the weight of the dry specimen same. **Figure 12** shows the effect of sintering time on the water absorption vs percentage of Al powder characters. The corresponding water absorption values are given in **Table 10**. It is found that the water absorption of

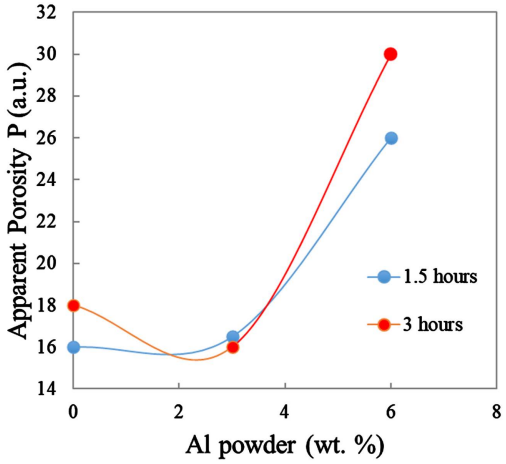

Figure 10. Apparent porosity of the glass-ceramics at different Al wt% for different sintering time.

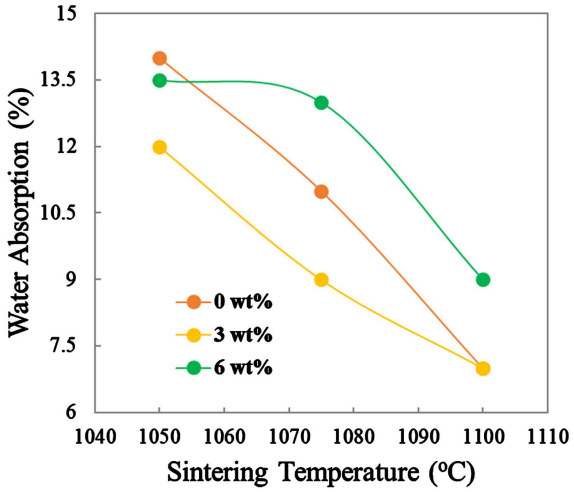

Figure 11. Water absorption characteristics of the glass-ceramics at different sintering temperature for different Al wt%.

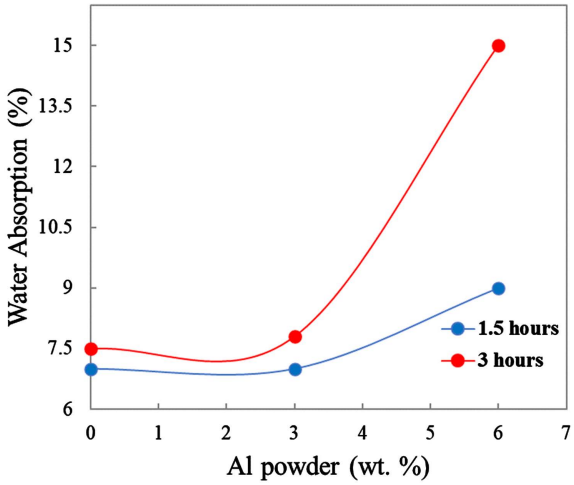

Figure 12. Water absorption characteristics of the glass-ceramics at different sintering temperature for different Al wt%.

Table 8. The value of the apparent porosity of the glass-ceramics at different Al wt% for different sintering time.

Al (wt%)	Apparent Porosity P (a.u.)	
	Sintered 1.5 h	Sintered 3 h
0	16	18
3	16.5	16
6	26	30

Table 9. Water absorption data of the glass-ceramics at different sintering temperature for different Al wt%.

Temperature (˚C)	Water Absorption (%)		
	Al (wt 0%)	Al (wt 3%)	Al (wt 6%)
1050	14	12	13.5
1075	11	9	13
1100	7	7	9

Table 10. Water absorption data of the glass-ceramic at different Al wt% added for different sintered time.

Al (wt%)	Water Absorption (%)	
	Sintered 1.5 h	Sintered 3 h
0	7	7.5
3	7	7.8
6	9	15

the sintered glass-ceramic samples increase (7% to 9%, and 7.5% to 15%) with increasing the sintering time from 1.5 hours to 3.0 hours.

4. Conclusion

We studied physical and mechanical properties of the Al-powder reinforced bioactive glass-ceramic composite material for bio-medical applications. We concluded the results for this investigation. It is observed that the flexural strength of the composites increased with increasing of Al powder added until a certain amount (>3 wt%). Similar results were obtained for the tangent modulus and flexural strain of the composites which increased with temperature for small amount of Al powder added, however decreased for higher amount of powder added (>3 wt%) with high temperature. Apparent porosity and water absorption of the composites decreased with increasing sintering time, temperature, and addition of Al powder. Although it is desirable to minimize the porosity to increase the resistance of the ceramics, the usefulness of this approach is limited. Therefore, further investigation is necessary in drawing a compromise relation

between the pore size and cellular integration into the materials. Optimization of the physicochemical characteristics for bone reconstruction should then be possible.

Conflicts of Interest

The authors declare no conflicts of interest regarding the publication of this paper.

References

[1] Buddy, D.R. and Stephanie, J.B. (2004) Biomaterials: Where We Have Been and Where We Are Going. *Annual Review of Biomedical Engineering*, **6**, 41-75. https://doi.org/10.1146/annurev.bioeng.6.040803.140027

[2] Williams, D.F. (1987) Definitions in Biomaterials. In: *Progress in Biomedical Engineering*, Elsevier, Amsterdam, Vol. 4, 72.

[3] Sakiyama-Elbert, S.E. and Hubbell, J.A. (2001) Functional Biomaterials: Design of Novel Biomaterials. *Annual Review of Materials Research*, **31**, 183-201. https://doi.org/10.1146/annurev.matsci.31.1.183

[4] Doremus, R.H. (1992) Bioceramics. *Journal of Materials Science*, **27**, 285-297. https://doi.org/10.1007/BF00543915

[5] Pizzoferrato, A., Marchetti, P.G., Ravaglioli, A. and Lee, A.J.C. (1986) Biomaterials and Clinical Applications. *Proceedings of the Sixth European Conference on Biomaterials*, Bologna, 14-17 September 1986, 186. http://hdl.handle.net/2027.42/27238

[6] Shah, A.T., Batool, M., Chaudhry, A.A., Iqbal, F., Javaid, A., Zahid, S., Ilyas, K., Qasim, S., Khan, A.F., Khan, A.S. and Rehman, I. (2016) Effect of Calcium Hydroxide on Mechanical Strength and Biological Properties of Bioactive Glass. *Journal of the Mechanical Behavior of Biomedical Materials*, **16**, 30050-30059. https://doi.org/10.1016/j.jmbbm.2016.03.030

[7] Soltesz, U. (1988) Ceramics in Composites. *Annals of the New York Academy of Sciences*, **523**, 137-156. https://doi.org/10.1111/j.1749-6632.1988.tb38508.x

[8] Boccardi, E., Ciraldo, F.E. and Boccaccini, A.R. (2017) Bioactive Glass-Ceramic Scaffolds: Processing and Properties. *MRS Bulletin*, **42**, 226-232. https://doi.org/10.1557/mrs.2017.28

[9] Serbena, F.C., Mathias, I., Foerster, C.E. and Zanotto, E.D. (2015) Crystallization Toughening of a Model Glass-Ceramic. *Acta Materialia*, **86**, 216-228. https://doi.org/10.1016/j.actamat.2014.12.007

[10] Montazerian, M., Singh, S.P. and Zanotto, E.D. (2008) An Analysis of Glass-Ceramic Research and Commercialization. *American Ceramic Society Bulletin*, **94**, 30-35. https://www.glassyage.com/wp-content/uploads/2020/08/5-An-analysis-of-glass-ceramic-research-and-commercialization.pdf

[11] Gerhardt, L.C. and Boccaccini, A.R. (2010) Bioactive Glass and Glass-Ceramic Scaffolds for Bone Tissue Engineering. *Materials*, **3**, 3867-3910. https://doi.org/10.3390/ma3073867

[12] Holand, W. and Beall, G.H. (2012) Glass-Ceramic Technology. 2nd Edition, John Wiley & Sons, Hoboken. https://doi.org/10.1002/9781118265987

[13] Montazerian, M. and Zanotto, E.D. (2016) History and Trends of Bioactive Glass-Ceramics. *Journal of Biomedical Materials Research*, **104**, 1231-1249.

https://doi.org/10.1002/jbm.a.35639

[14] Phillips, D.C., Sambell, R.A.J. and Bowen, D.H. (1972) The Mechanical Properties of Carbon Fibre Reinforced Pyrex Glass. *Journal of Materials Science*, **7**, 1454-1464. https://doi.org/10.1007/BF00574937

[15] Prewo, K.M. and Brennan, J.J. (1980) High-Strength Silicon Carbide Fibre-Reinforced Glass-Matrix Composites. *Journal of Materials Science*, **15**, 463-468. https://doi.org/10.1007/BF02396796

[16] Venkatesh, R. and Chawla, K.K. (1992) Effect of Interfacial Roughness on Fibre Pull-Out in Alumina/SnO_2/Glass Composites. *Journal of Materials Science*, **11**, 650-652. https://doi.org/10.1007/BF00728894

[17] Ye, F., Yang, J., Zhang, L., Zhou, W., Zhou, Y. and Lei, T. (2001) Fracture Behavior of SiC-Whisker-Reinforced Barium Aluminosilicate Glass-Ceramic Matrix Composites. *Journal of the American Ceramic Society*, **84**, 881-883. https://doi.org/10.1111/j.1151-2916.2001.tb00759.x

[18] Ye, F., Liu, L., Wang, Y., Zhou, Y., Peng, B. and Meng, Q. (2006) Preparation and Mechanical Properties of Carbon Nanotube Reinforced Barium Aluminosilicate Glass-Ceramic Composites. *Scripta Materialia*, **55**, 911-914. https://doi.org/10.1016/j.scriptamat.2006.07.045

[19] Sarkar, P., Modak, N. and Sahoo, P. (2017) Mechanical Characteristics of Aluminium Powder Filled Glass Epoxy Composites. *International Journal of Engineering and Technologies*, **12**, 1-14. https://doi.org/10.18052/www.scipress.com/IJET.12.1

[20] Annual Book of ASTM Standards, Part 17 (1979) Refractories, Glass, and Other Ceramic Materials. https://www.worldcat.org/title/1979-annual-book-of-astm-standards-pt-17-refractories-glass-and-other-ceramic-materials-manufactured-carbon-and-graphite-products/oclc/6937310

[21] Zweben, C., Smith, W. and Wardle, M. (1979) Test Methods for Fiber Tensile Strength, Composite Flexural Modulus, and Properties of Fabric-Reinforced Laminates. *Composite Materials*: *Testing and Design* (*Fifth Conference*), New Orleans, 20-22 March 1978, 228-262. https://doi.org/10.1520/STP36912S

[22] Brenan, J.J. and Prewo, K.M. (1982) Silicon Carbide Fibre Reinforced Glass-Ceramic Matrix Composites Exhibiting High Strength and Toughness. *Journal of Materials Science*, **17**, 2371-2383. https://doi.org/10.1007/BF00543747

[23] Taskiran, M.U., Demirkol, N. and Capoglu, A. (2006) Influence of Mixing/Milling on Sintering and Technological Properties of Anorthite Based Porcelainised Stoneware. *Ceramics International*, **32**, 325-330. https://doi.org/10.1016/j.ceramint.2005.03.010

[24] Jiang, F., Zhang, L., Jiang, Z., Li, C., Cang, D., Liu, X., Xuan, Y. and Ding, Y. (2018) Diatomite-Based Porous Ceramics with High Apparent Porosity: Pore Structure Modification Using Calcium Carbonate. *Ceramics International*, **45**, 6085-6092. https://doi.org/10.1016/j.ceramint.2018.12.082

[25] Tognonvi, M., Tagnit-Hamou, A., Konan, L., Zidol, A. and N'Cho, W. (2020) Reactivity of Recycled Glass Powder in a Cementitious Medium. *New Journal of Glass and Ceramics*, **10**, 29-44. https://doi.org/10.4236/njgc.2020.103003